JPET Fast Forward. Published on July 10, 2007 as DOI: 10.1124/jpet.107.126409
This article has not been copyedited and formatted. The final version may differ from this version.

JPET#126409

Title Page

Effects of endogenous ascorbate on oxidation, oxygenation and toxicokinetics of cell-free modified hemoglobin after exchange transfusion in rat and guinea pig

Paul W. Buehler, Felice D'Agnillo, Victoria Hoffman and Abdu I Alayash

Laboratory of Biochemistry and Vascular Biology, Division of Hematology, Center for Biologics Evaluation and Research (CBER), Food and Drug Administration (FDA), Bethesda, Maryland 20892, USA (P.W.B, F.D., A.I.A.)

Division of Veterinary Services, Office of the Center Director, National Institutes of Health, Bethesda, Maryland 20892, USA (V.H.)

Running Title Page

Running Title: Plasma reductive capacity and Hb oxygen and redox kinetics

Correspondence:

Paul W. Buehler Pharm.D, Ph.D., CBER, FDA

8800 Rockville Pike, Bldg. 29, Rm. 129

Bethesda, MD 20892

Telephone: (301) 451-3953; E-Mail: paul.buehler@fda.hhs.gov

Fax: (301) 435-4034

Number of text pages: 43

Number of figures: 9

Number of references: 33

Number of words in abstract: 239

Number of words in introduction: 764

Number of words in discussion: 1,752

Abbreviations: Hb, hemoglobin; ET, exchange transfusion; bovine polymerized hemoglobin, PolyHbBv; AA, ascorbic acid; OEC, oxygen equilibrium curve; HIF-1α, hypoxia inducible factor; HBOC, hemoglobin based oxygen carrier; NO, nitric oxide; LGO, L-gulonolactone oxidase; SOD, superoxide dismutase; DHA, dehydroascorbate; MALDI-MS, matrix assisted laser desorption ionization mass spectrometry; $AUC_{0-\infty,}$ area under the plasma concentration time curve; C_{last}, last measurable concentration; CL, plasma clearance; MRT , mean residence time; $V_{ss,}$ apparent volume of distribution; $t_{1/2,}$ half-life

Abstract

Chemically modified hemoglobin (Hb) solutions are promising oxygen therapeutics, however, these agents are prone to intravascular oxidation. Using a 50% exchange transfusion (ET) model with bovine polymerized hemoglobin (PolyHbBv), we examined heme oxidation, oxygenation markers and toxicokinetics in rats, an ascorbic acid (AA) producing species, and guinea pigs, a non-AA producing species. Plasma AA decreased by 50% in guinea pigs after ET but was unchanged in rats for the first 20 hours post ET. Both species cleared PolyHbBv from the circulation at similar rates. However, exposure to ferric PolyHbBv over time was five-fold greater in the guinea pig. Mass spectrometry analysis of plasma revealed oxidative modifications within the tetrameric fraction of PolyHbBv in guinea pig. Oxygen equilibrium curves (OECs) of PolyHbBv measured in plasma after ET were more left shifted in guinea pigs compared to rats consistent with increased ferric PolyHbBv formation. Renal hypoxia-inducible factor (HIF-1α), whose activity strictly depends on P_{O2} increased over time and correlated inversely with circulating ferrous PolyHbBv in both species. Interestingly, HIF-1α activity was greater in guinea pigs compared to rats at 72 hours post ET. Mean arterial pressure increases were also greater in guinea pigs, however, minimal differences in cardiac and renal pathology were observed in either species. The present findings suggest the importance of plasma AA in maintaining the stability of therapeutic agents susceptible to oxidation and may be relevant to humans which display a similar plasma/tissue antioxidant status to guinea pig.

Introduction

Hemoglobin (Hb) based oxygen carriers (HBOCs) represent a class of complex biologic entities being developed as oxygen bridging agents with volume expanding properties. Despite their therapeutic promise, HBOCs demonstrate a significant potential for toxicity based on administration of large quantities of Hb into the plasma compartment. Normally Hb remains protected in the red blood cell where processes exist to reduce oxidized Hb and modulate nitric oxide (NO) binding. It has become increasingly evident that Hb oxidative toxicity can limit the safety and efficacy of current generation HBOCs (Alayash, 2004). This prompted the design of new strategies aimed at reducing or controlling Hb-oxidative side reactions. *In vivo* oxidation of cell-free Hb is driven spontaneously and/or chemically by variety of oxidants including hydrogen peroxide (H_2O_2) and NO. NO-induced oxidation of heme iron has the added complication of producing an immediate elevation in blood pressure as a result of removal of NO (a vasodilator) by Hb. Thus, two primary safety concerns with HBOCs in the extra-cellular space include hypertension and oxidative stress (Riess, 2001; Alayash, 2004). The latter depends on plasma and tissue reductive capacity to maintain the HBOC in a reduced and functional state.

HBOCs have generally demonstrated promising safety and efficacy in animals and, in many cases, favorable Phase I clinical safety (Przybelski R et al., 1996; Carmichael FJ et al., 2000). However, recent well-publicized late Phase clinical trial failures with certain

HBOCs suggest that preclinical animal testing may not have been sufficiently predictive of safety in humans (Sloan EP et al., 1999; Greenberg AG and Kim HW et al., 2004). This recognition has highlighted the need for improved animal models and biomarkers to better predict and monitor the safety and efficacy of HBOCs in humans. In this regard, the selection of animal species to evaluate HBOCs is critical for predicting safety in both normal and disease state human subjects.

In the present study, we compare the rat, recognizing its popularity as a small animal species used in non-clinical HBOC studies and the guinea pig as a potentially more relevant small animal species for predicting human safety. The rationale for evaluating the guinea pig is based on several factors which suggest a similarity with humans in terms of overall antioxidant status. Guinea pigs like humans are incapable of endogenous production of ascorbic acid (AA) due to the evolutionary loss of functional hepatic L-gulonolactone oxidase (LGO). In contrast, rats generate 38 μg AA/mg LGO/hr under normal conditions and even greater amounts when subjected to stress (Chatterjee IB, 1973). Interestingly, extensive investigations of several HBOCs in non-clinical studies often involving AA producing species such as rat and swine have demonstrated acceptable safety profiles.

Guinea pigs and humans appear to have compensated for the lack of endogenous AA production by increasing tissue antioxidant enzyme content and efficiency, for example copper and zinc superoxide dismutase (SOD) enzymatic activity in kidney and liver is approximately two fold higher in humans and guinea pigs compared to rats (Nandi A et

al., 1997). More recently human and guinea pig but not rat red blood cells have been found to possess a similar oxidorecutase system, cytochrome b561, responsible for efficiently recycling dehydroascorbate (DHA) to functional AA (Su D et al., JBC 2006). Therefore, the general antioxidant status of guinea pig and human are quite similar such that the balance of reductive capacity is tilted toward the tissue and away from the plasma in guinea pigs and humans. Germane to these similarities is that plasma antioxidant capacity is necessary for maintaining HBOCs in a reduced form such that they are able to carry and deliver oxygen efficiently, maintain heme stability and limit toxicity. This is especially important when tissue antioxidant status is diminished during hemorrhagic shock and ischemic conditions.

In the current study, rats and guinea pigs were subjected to 50% exchange transfusion with bovine polymerized hemoglobin (Oxyglobin®, PolyHbBv), an FDA approved HBOC for veterinary use. We identified a strong correlation between plasma AA levels and the susceptibility of PolyHbBv to undergo oxidation and correlated these events for the first time with tissue oxygen sensing mechanisms. Despite dramatic inter-species differences in plasma PolyHbBv oxidation and stability, minimal differences were found when comparing the overall effect on cardiac and renal pathology, which may reflect differences in local tissue antioxidative mechanisms. These data are consistent with the general safety of certain HBOCs in normal human subjects treated in early phase clinical trials. However, more extensive work using the guinea pig in models of tissue compromise (e.g. ischemia/reperfusion) when tissue oxidative status is reduced may ultimately provide answers to why certain HBOCs fail in pivotal clinical trials.

Methods

Solutions: Oxyglobin® (PolyHbBv) was purchased from Biopure Corporation (Cambridge, MA). This solution consists of a heterogeneous mixture of glutaraldehyde polymerized bovine hemoglobin at a concentration of 13 g/dL in modified Lactated Ringer's. A detailed description of the physicochemical properties of the mixture as a whole and each individual fraction has been described elsewhere (Alayash et al., 2001; Buehler PW et al., 2005).

Animals and surgical preparation: Male Sprague-Dawley rats and Hartley guinea pigs were purchased from Charles Rivers Laboratories (Wilmington, MA) and acclimated for 1 week upon arrival to the FDA/Center for Biologics Evaluation and Research (CBER) animal care facility. All animals were fed normal diets throughout the acclimation period and weighed 350-450 g at the time of study. Animal protocols for each species were approved by the FDA/CBER Institutional Animal Care and Use Committee with all experimental procedures performed in adherence to the National Institutes of Health guidelines on the use of experimental animals.

On days of surgery, rats and guinea pigs were anesthetized via the i.p. route with a cocktail of ketamine HCl (100 mg/kg) and xylazine HCl (5 mg/kg) (Phoenix Scientific Inc., St. Joseph, MO). Under aseptic conditions a midline incision was made around the neck region allowing for blunt dissection and exposure of the right common carotid

artery and the left external jugular vein. Saline filled catheters containing 50 IU of heparin per mL prepared from sterile PE50 tubing (Clay Adams of Becton-Dickenson, Sparks, MD) were placed in each vessel and tunneled under the skin to the back of the neck. Immediately following surgeries animals were administered a subcutaneous dose of buprenorphine (0.1 mg/kg) (Reckitt and Coleman Corp., Kingston, UK) and allowed 24 hours of recovery prior experimentation. For blood pressure measurements the right femoral artery was also catheterized with PE10 tubing fused to PE50 tubing to allow for simultaneous administration of PolyHbBv and monitoring of arterial blood pressure. The right carotid artery catheter was connected to a Gould P23 XL pressure transducer (Gould Instrument System Inc., Valley View, OH) for recording blood pressure. Arterial blood pressure was recorded continuously at 100 Hz using a MP100A-CE data acquisition system (Biopac Systems, Inc., Santa Barbara, CA). Data were analyzed off-line using AcqKnowledge software (Biopac Systems, Inc., Santa Barbara, CA) to determine mean arterial pressure (MAP) from the following formula [diastolic + 1/3 (systolic – diastolic)] with each being averaged over consecutive minutes of acquired data.

Blood/tissue collection: 350 μL of blood was sampled (before infusion), immediately after infusion, and at 4, 12, 24, 48 and 72 hrs after end of ET for the following analyses: (1) plasma AA (2) hematocrit (HCT); (3) plasma oxygen equilibrium values. Heart and kidneys were harvested at the same time points for histopathology and renal HIF activity. Each time point represents an n=3-5 animals.

In a separate group of animals (n=5-6) blood samples (0.2 mL) were obtained from the arterial catheter prior to infusion (baseline) and at the end of ET (time 0), and at 0.25, 0.5, 1, 1.5, 2, 2.5, 3, 4, 8, 12, 24, 48 and 72 hours after the end of ET. Plasma was used for evaluation of (1) total PolyHbBv, (2) ferrous PolyHbBv, (3) ferric PolyHbBv and (4) PolyHbBv polymeric component distribution.

Plasma ascorbic acid analysis: Plasma AA was analyzed by a modified reverse phase HPLC method. Briefly, plasma samples (200 μL) were centrifuge filtered at 12,000 rpm for 45 minutes at 4°C using microcon YM-10 filter tubes (Millipore, Bedford, MA) to remove PolyHbBv and other proteins greater than 10,000 Da. Standard curves and controls were prepared in normal saline using AA (Sigma Chemical Co., St. Louis, MO) and acetaminophen (Sigma Chemical Co., St. Louis, MO) as the internal standard. All standards and controls were subjected to the same filtration steps. Total AA (oxidized and reduced AA) was evaluated by adding 5 μL of a 100 mM solution of dithiothreitol (DTT) (Sigma Chemical Co., St. Louis, MO) to each filtered sample to reduce any dehydroascorbic acid (DHA). Standards and samples (50 μL) were run on a PrimeSep D (4.6x100mm, 5um) reverse phase column with a PrimeSep D (4.6x10mm) guard column (SIELC Technologies, Inc. Prospect Heights, IL) attached to a Dionex Summit P680 Pump with a Dionex UVD 170S detector (Dionex Corp., Sunnyvail, CA). The mobile phase consisted of 40% AcCN/1% acetic acid and was pumped at a rate of 1 mL/min. Absorbance was measured at 254 nm for detection of AA and acetaminophen.

Pharmacokinetic/toxicokinetic analysis: Fully conscious and freely moving rats (n=6) and guinea pigs (n=5) underwent a 50% ET replacing blood with PolyHbBv. Arterial and venous catheters were extended, tethered and connected to separate syringe pumps (Model 11 Harvard Apparatus, Holliston, MA) set on withdrawal (1 mL/min) and infuse (1 mL/min), respectively. 50% ET volume in the rat was calculated as 50% ET (mL) = [0.06 (mL/g) x body weight (g) + 0.77] / 2 (Lee and Blaufox , 1985) and as 50% ET (mL) = [0.07 (mL/g) x body weight (g)] / 2 in the guinea pig (Ancill, 1956). Plasma from blood in the heparinized withdrawal syringe for each transfused animal was obtained to determine the total PolyHbBv removed during the exchange transfusion period (approximately 12 minutes). Blood samples (0.2 mL) were obtained from the arterial catheter prior to infusion (baseline) and at the end of ET (time 0), 0.25, 0.5, 1, 1.5, 2, 2.5, 3, 4, 8, 12, 24, 48 and 72 hours.

Plasma concentrations of ferrous PolyHbBv and ferric PolyHbBv were determined using a photodiode array spectrophotometer (Model 8453 Hewlet Packard, Palo Alto, CA). Plasma from the baseline (pre-ET) sample for each animal was used to correct for background interference and turbidity. Concentrations of ferrous PolyHbBv (oxy/deoxy), ferric PolyHbBv and hemichrome were determined using a multi-component analysis based the extinction coefficients for each Hb species (Winterbourn, 1985). Electron paramagnetic resonance (EPR) was also used to confirm that ferric PolyHbBv in the circulation was primarily in its non-liganded state as opposed to partially liganded or fully liganded (e.g. Fe^{3+}- NO) forms which are indistinguishable by UV-Vis spectrophotometry (data not shown).

JPET Fast Forward. Published on July 10, 2007 as DOI: 10.1124/jpet.107.126409
This article has not been copyedited and formatted. The final version may differ from this version.

Pharmacokinetic analysis: The dose (mg) of PolyHbBv received by each animal at the end of ET was determined by subtracting the total amount of PolyHbBv in the plasma from whole blood collected in the ET syringe from the total amount of infused PolyHbBv according to the following equation:

$$dose_{received} = ([PolyHbBv]_{\inf} \times V_{\inf}) - ([PolyHbBv]_{totalET} \times V_{ET})$$

Where dose $[PolyHbBv]_{inf}$ is the concentration of PolyHbBv (mg/mL) infused, V_{inf} is the PolyHbBv infusion volume (mL), $[PolyHbBv]_{totalET}$ is the concentration of PolyHbBv (mg/mL) from plasma sampled out of the withdrawal syringe and V_{ET} is the volume (mL) collected in the withdrawal syringe. MALDI-MS was performed to confirm that no Hb originating from red blood cells (RBC) was present in the withdraw syringe sampled plasma. MALDI-MS was also performed on both rat and guinea pig plasma to explore stability of circulating PolyHbBv fractions, described later.

PK parameters were determined for total PolyHbBv, ferrous PolyHbBv (oxy/deoxy) and ferric PolyHbBv. Noncomparmental methods employed by WinNonlin version 4.1 (Pharsight Corp., Mountain View, CA, USA) were used to calculate PK parameter estimates. The area under the plasma concentration time curve ($AUC_{0-\infty}$) was estimated using the linear trapezoidal rule to the last measurable concentration ($AUC_{0-C\ last}$). Extrapolation to infinity ($AUC_{C\ last-\infty}$) was accomplished by dividing C_{last} by the negative value of the terminal slope (k) of the log-linear plasma concentration-time curve. Thus $AUC_{0-\infty}$ is equal to the sum of $AUC_{0-C\ last}$ and $AUC_{C\ last-\infty}$. Additional parameters were calculated as follows: Plasma clearance (CL) as dose divided by $AUC_{0-\infty}$, mean residence

time (MRT) as k^{-1}, apparent volume of distribution (V_{ss}) as the product of CL and MRT and half-life ($t_{1/2}$) as the product of ln2 and MRT.

Plasma oxygen equilibrium curve (OEC) measurements: Oxygen equilibrium curves were obtained using a Hemox analyzer (TCS Scientific, New Hope, PA). Experiments were carried out in 0.1 M phosphate buffer/0.1 M NaCl at a pH 7.4 and the temperature was maintained at 37 °C. To prevent formation of ferric PolyHbBv, 4 μL of the Hayashi enzymatic reduction system was added to the 4 mL solution (Hayashi et al., 1973). Oxygen equilibrium parameters were derived by fitting the Adair equations to each OEC by the non linear least squares procedure included in the Hemox analyzer software (p50 PLUS, version 1.2) (Alayash et al., 2001). The Adair constants were then used to generate an OEC curve to generate the P_{50} and n_{50} (Hill coefficient) for oxygen binding. Therefore, the procedure made it possible to measure the oxygen binding parameters of PolyHbBv, which is not fully saturated at atmospheric oxygen partial pressures (Nagababu E et al., 2002).

PolyHbBv polymer distribution and globin chain dissociation in plasma: Plasma samples (50 uL) were evaluated by size exclusion chromatography (SEC) to compare distribution of HbG polymeric components at time points post ET. Samples were run on a BioSep-SEC-S3000 (600 mm x 7.5 mm) SEC column (Phenomenex, Torrance, CA) attached to a Waters 626 pump and Waters 2487 dual-wavelength detector, controlled by a Waters 600s controller using Millenium32 software (Waters Corp., Milford, MA). The running

buffer consisted of 0.1 M NaH_2PO_4, pH 6.5, pumped at rate of 0.5 mL/min and the absorbance was monitored at 405 nm.

Plasma samples (10 uL) were desalted using C18 ZipTips (Millipore, Bedford, MA) according to the manufacturer's instructions. A 1 μL aliquot was pipetted onto a stainless steel MALDI-MS sample plate and mixed with 1 μL of 3,5-dimethoxy-4-hydroxycinnamic acid (sinapinic acid) (Sigma Chemical Co., St. Louis, MO) saturated in 50% Acetonitrile (AcCN)/ 0.1% trifluroacetic acid (TFA). The sample/matrix was air dried and analyzed on a PerSeptive Biosystems DERP MALDI-TOF mass spectrometer calibrated manually with purified human serum albumin (Sigma Chemical Co., St. Louis, MO) and using Voyager 5.1 software with Data Explorer (Applied Biosystems, Framingham, MA) operated in linear mode.

Blood Pressure: Fully conscious and freely moving rats (n=5-6) and guinea pigs (n=5-6) underwent a 50% exchange transfusion (ET) replacing blood with PolyHbBv (13 g/dL). Withdrawal of blood and infusion of PolyHbBv took place simultaneously at a rate of 1 mL/min from the right femoral artery and the left external jugular vein, respectively. The right carotid artery catheter was connected to a Gould P23 XL pressure transducer (Gould Instrument System Inc., Valley View, OH) for recording blood pressure. Arterial blood pressure was recorded continuously at 100 Hz using a MP100A-CE data acquisition system (Biopac Systems, Inc., Santa Barbara, CA). Data was analyzed off-line using AcqKnowledge software (Biopac Systems, Inc., Santa Barbara, CA) to determine mean

arterial pressure (MAP) from the following formula [diastolic + 1/3 (systolic – diastolic)] with each being averaged over consecutive minutes of acquired data.

Hypoxia-inducible factor-1α DNA binding assay: HIF-1 α DNA binding activity of animal tissues was determined by using an ELISA-based method (Transbinding HIF-1α Assay kit) from Panomics (Redwood City CA) according to manufacturer's specifications. HIF-1 α transcriptional factor was assessed by detection of its binding to an oligonucleotide containing the hypoxia-responsive element (5`-TACGTGCT-3`) after lysis, and nuclear extraction was achieved with the use of a nuclear extraction kit provided by manufacturer. HIF-1α binding was detected by a mouse antibody directed against HIF-1α region available after DNA binding and revealed by ant-mouse IgG coupled to horseradish peroxidases (HPR) which provides sensitive colorimetric detection by a spectrophotometric microplate reader at 450 nm.

Histopathology: Hearts and kidneys were fixed in 10% formalin, embedded in paraffin, and 5 μm sections were cut and stained by standard hematoxylin-eosin (H/E) procedures. Tissues were scored by a veterinary pathologist using a semiquantitative grading system as follows: 0=minimal, 1=mild, 2=moderate, 3=severe (minimal- indicates a detectable process but barely present, mild- small aggregates of inflammatory or necrotic cells, moderate- large aggregated inflammatory or necrotic cells at 20X and severe- large multi-focal aggregates making up greater than 50% of the tissue area).

Statistical Analysis: Arterial blood pressures, heart rate, non-compartmental analyses of PK parameter estimates, hematocrit and plasma ascorbate concentrations are expressed as means ± SEM. Statistical comparison for arterial blood pressures, heart rate, PK parameter estimates, hematocrit and plasma AA concentrations were performed by ANOVA with an a priori test for planned comparisons between the rat and the guinea pig. In all analyses, a value $p < 0.05$ was taken as the level of statistical significance.

Results

Plasma AA levels following exchange transfusion: Plasma reductants such as AA have been shown to effectively reduce oxidized Hb in humans (Ames B et al., 1981). Figure 1A shows plasma AA concentrations in rats and guinea pigs following 50% ET. Baseline (BL) plasma AA concentrations in the rat and guinea pig were 100.03 ± 16.2 μM and 51 ± 15.8 μM, respectively. When subjected to 50% ET, rats exhibited plasma AA concentrations similar to BL at 4 hours (97.2 ± 5.2 μM), 12 hours (104.6 ± 7.0 μM) and 24 hours (109.4 ± 21 μM) post ET. At 48 hours post ET, plasma AA concentration decreased below BL (i.e., 51.6 ± 13 μM) and this AA concentration was maintained at 72 hours post ET (50.8 ± 17 μM). An opposite situation occurred in guinea pigs following 50% ET such that AA plasma concentrations were approximately 50% of BL at 4 hours (22 ± 5.7 μM), 30% of BL at 12 hours (15.9 ± 3.4 μM), 36% of BL at 24 hours (18.5 ± 5.8 μM), 41% of BL at 48 hours (20.9 ± 3.1 μM) and 96% of BL at 72 hours (48.1 ± 16 μM) post ET. These data suggest that the rat rapidly up-regulates AA hepatic production to make up for losses during ET, while in the guinea pig a 50% loss of AA plasma

concentration is observed 4 hours after 50% ET and remained low which is consistent with a 50% exchange transfusion in a species incapable of endogenous AA production.

Efficient AA functioning is dependent on the presence of normal circulating red blood cells (RBCs) which chemically recycle dehydroascorbic acid (DHA) back to functional AA (May JM et al., 2004). Given this intimate relationship between AA and RBCs, hematocrit (Hct) levels in the two species were also measured (Fig. 1B). Baseline Hct levels were 44.4 ± 1.5 and 37.8 ± 0.85 percent in the rat and guinea pig, respectively, while ET reduced Hct levels to 21.9 ± 0.92 and 18.3 ± 0.47 in each species. Over the 72 hours of evaluation neither species demonstrated changes in Hct from end ET levels. These results indicate that the exchange transfusion resulted in similar reductions in red cell volume in both species and thus red cell volume can not account for the inter-species differences in plasma AA.

*Ferric PolyHbBv formation following exchange transfusion***:** To examine the possible correlation between plasma AA levels, oxidation and oxidative stability of PolyHbBv, we measured the post-exchange levels of ferric PolyHbBv (Fig. 2). The C_{max} for ferric PolyHbBv occurred at time zero (end of ET) in the rat and at 12 hours post ET in the guinea pig accounting for 2.2 % and 23.2 % of the total PolyHbBv concentration in each species at each T_{max}, respectively. The $AUC_{0-\infty}$ for ferric PolyHbBv in the rat and guinea pig was 6.6 % and 34.5 % of the total PolyHbBv $AUC_{0-\infty}$, respectively. Plasma CL of ferrous PolyHbBv occurred faster in the guinea pig compared to the rat, however no such difference was found in total PolyHbBv plasma CL.

The critical period of ferric PolyHbBv exposure in the guinea pig appears to exist between the 4 and 48 hour post ET time points when total PolyHbBv plasma concentrations are 19.5 g/dL and 8.0 g/dL, respectively. Between these time points, the % ferric PolyHbBv in the plasma ranged from 10.7 % (4 hours) to 40 % (36 hours). By 72 hours post ET, the plasma concentrations of total PolyHbBv were less than 5% of the C_{max} thus the % of total PolyHbBv as ferric PolyHbBv becomes small and of minimal relevance. In the rat, % ferric PolyHbBv is ≤ 5% of the total PolyHbBv concentration between the end of ET until 24 hours post ET. At 48 hours post ET, total PolyHbBv is approximately 0.4 g/dL with 18% of this concentration as ferric PolyHbBv. By 72 hours post ET, the plasma concentration of total PolyHbBv is less than 5% of the C_{max} thus the % of total PolyHbBv as the oxidized (ferric) form is negligible. These data suggest that oxidative processes are likely responsible for the greater formation of plasma ferric PolyHbBv in guinea pigs rather than increased whole body CL of ferrous PolyHbBv. Moreover, these findings identify the rat as a species that can prevent the physiological accumulation of ferric PolyHbBv within the plasma compartment, while the guinea pig may more accurately reflect plasma accumulation of ferric PolyHbBv in other non AA producing species (i.e. humans).

Pharmacokinetic analysis:

Table 1 shows the pharmacokinetic parameter estimates for total PolyHbBv, ferrous PolyHbBv and ferric PolyHbBv following a 50% PolyHbBv for blood ET. Rats and guinea pigs received 3122 ± 55 mg/kg and 3272 ± 106 mg/kg doses of PolyHbBv,

respectively. This dosing level is representative of a high single administration of PolyHbBv equal to 7 units in a 70 kg adult human or 220 g of cell free PolyHbBv. At time zero (end of ET), plasma concentrations of PolyHbBv in both species were comprised of 94 % ferrous PolyHbBv and 6% ferric PolyHbBv. (Fig. 2) shows the data used to define non-compartmental parameter estimates plotted as log mean ± sem (<5% of mean values) plasma concentration versus time. The Vss for PolyHbBv was approximately 2-2.5 times greater in each species than the expected circulating blood volume following a 50% ET with an oncotically matched solution (i.e. colloid osmotic pressure equal to blood). Although not directly measured in this study, data suggests an increase in circulating vascular volume and a rapid saturating non-specific tissue distribution. In both species, increased urination and hematuria was observed during the 50% ET and in the initial four hours of observation post ET. The total PolyHbBv estimates for t½ and MRT were similar between species. The primary exposure parameters (C_{max}, $AUC_{0-\infty}$) and total CL demonstrated species similarity for total PolyHbBv following dosing in the rat and guinea pig. However, when the oxidation state of PolyHbBv was accounted for in the PK analysis, ferrous PolyHbBv and ferric PolyHbBv exposure parameter differences between the rat and guinea pig became evident.

Plasma PolyHbBv component plasma distribution/globin chain dissociation:

The SEC chromatographs of plasma from rat and guinea pig obtained from blood samples at the end of ET until 72 hours post ET were separated on a BioSep-SEC-S3000 (600 mm x 7.5 mm) SEC column (Phenomenex, Torrance, CA) are shown in (Fig. 3 A

and B). As expected the chromatograms show a more rapid loss of tetramer in each species and a slower disappearance of multi-tetrameric PolyHbBv components. PolyHbBv tetramer and multi-tetrameric species appear to be similarly eliminated from the plasma at time points post ET. Alternatively, larger PolyHbBv multi-tetramers may break down to smaller M.W. components prior to elimination. However, upon closer inspection of PolyHbBv elimination curves and SEC chromatograms obtained from guinea pig plasma both PolyHbBv tetrameric and multi-tetrameric fractions appear to be eliminated more rapidly in the first four hours post ET. This observation may be due to the accelerated oxidation of PolyHbBv in guinea pigs and thus increased elimination may serve as an early protective mechanism removing oxidized PolyHbBv.

Structural and oxidative stability of PolyHbBv:

While tetramer stability is not evident from the SEC chromatograms, MALDI-MS analysis of plasma collected at 4 and 24 hours suggest that tetramers of PolyHbBv remain stable in the rat, but become unstable in the guinea pig circulation (representative spectra shown in Fig. 4, A and B). In (Fig. 4 A), the MALDI-MS spectra of rat RBC Hb demonstrates a α globin chain $[M+H]^{1+}$ ion at m/z = 15201.60 and a β globin chain $[M+H]^{1+}$ ion at m/z = 15851.51. These ions predominate even though rat Hb exists as multiple α and β globin chain variants (Garrick et al., 1975). At 4 and 24 hours post ET, the cross-linked PolyHbBv derived α globin chains are seen as an α*-α* $[M+H]^{1+}$ ion with an m/z = 30940.17, while residual α* $[M+H]^{1+}$ (limited % intensity) and intense β* $[M+H]^{1+}$ globin chain ions are observed at an m/z = 15285.00 and 16108.70, respectively. The cross-linked α globin chain ions suggest non-site specific modification

by glutaraldehyde (Buehler PW et al., 2005). The α* $[M+H]^{1+}$ ion region of the 24 hour plasma sample indicates no peak intensity change from the 4 hour sample suggesting limited tetramer destabilization *in vivo*.

In Figure 4B, the MALDI-MS spectra of guinea pig RBC Hb demonstrates an α globin chain $[M+H]^{1+}$ ion at m/z = 15228.59 and β globin chain $[M+H]^{1+}$ ion at m/z = 15921.00. The α and β globin chain ions are consistent with those reported in the literature (Day BW, Jin R, Karol MH. Chem. Res. Toxicol. 1996, 9, 568-573). At 4 and 24 hours post ET, the cross-linked PolyHbBv derived α globin chains are seen as an α*-α* $[M+H]^{1+}$ ion at an m/z = 31025.19, while residual α* $[M+H]^{1+}$ (limited % intensity) and intense β* $[M+H]^{1+}$ globin chain ions are observed at an m/z = 15250.81 and 16125.87, respectively. The α* $[M+H]^{1+}$ ion at a m/z = 15250.81 in the spectra of the 24 hour plasma sample indicates increased peak intensity of 35% from the 4 hour sample suggesting α globin chain cross-link destabilization *in vivo*. Rat and guinea pig plasma samples did not demonstrate mass ions for Hb's α or β globin chains originating from rat or guinea pigs own RBC. Thus destabilized α globin could only have come from PolyHbBv.

Blood pressure and heart rate response to PolyHbBv*:* HBOC-mediated blood pressure elevation is a common finding in animals and humans and can result in reduced tissue oxygenation. To investigate the possible relationship between PolyHbBv oxidative stability and the susceptibility and/or extent of hemodynamic alterations, we monitored blood pressure and heart rate in fully conscious and freely moving rats and guinea pigs

(n=5 for both) during the course of the 50% ET. (Fig. 5A) shows the changes in mean arterial pressure (MAP) between rat and guinea pig. Baseline blood pressure values monitored over 20 minutes in rats ranged as follows: systolic (140.4 ± 6.44 to 143.8 ± 6.40 mmHg), diastolic (109.6 ± 4.93 to 125.2 ± 6.22 mmHg), MAP (119.0 ± 5.81 to 125.2 ± 6.22 mmHg) and pulse pressure (23.8 ± 4.41 to 27.4 ± 2.11 mmHg). In guinea pigs, baseline blood pressure values ranged as follows: systolic (73.4 ± 3.60 to 83.2 ± 5.35 mmHg), diastolic (48.8 ± 4.85 to 56.2 ± 5.76 mmHg), MAP (60.2 ± 4.14 to 63.0 ± 4.10 mmHg) and pulse pressure (23.8 ± 4.41 to 27.4 ± 2.11 mmHg). Immediately after the start of ET, a concomitant drop in heart rate occurred (Fig. 5B).

The onset of ET resulted in immediate responses in all hemodynamic parameters measured in both species. The end of the 50% ET (approximately 10 minutes) resulted in the following blood pressure changes in the rat: systolic 157.4 ± 6.83 mmHg (12 % > BL), diastolic 115.6 ± 4.3 mmHg (6 % > BL), MAP 136.4 ± 7.10 mmHg (11 % > BL) and pulse pressure 41.8 ± 3.3 mmHg (75 % > BL. The overall arterial blood pressure elevation (systolic, diastolic and MAP) was greater in the guinea pig versus the rat. Interestingly the increase in MAP (diastolic + [(1/3) systolic – diastolic] in the rat was predominantly driven by an elevation in systolic pressure while diastolic pressure remained similar to baseline.

Plasma oxygen equilibrium curve analysis: The impact of increased plasma PolyHbBv oxidation on PolyHbBv oxygen-carrying capacity in both species was examined. Oxygen equilibrium curves (OEC) in plasma samples obtained over the course of 72 hours are

shown in (Fig. 6A and B) for rat and guinea pig respectively. From plasma OECs, we were able to calculate a P_{50} = 36.4 ± 0.989 mmHg immediately after the end of ET in the guinea pig compared to 41.7 ± 0.73 mmHg in the rat. At 48 hours post ET, a greater shift toward increased oxygen affinity (reduced oxygen off-loading) was observed in the guinea pig (P_{50} = 25.1 ± 0.441 mmHg) compared to the rat (38.9 ± 2.72 mmHg). These observations are consistent with the increased ferric PolyHbBv accumulation over time in guinea pigs.

Modulation of tissue hypoxia-inducible factor (HIF-1α) activity by PolyHbBv:

As an indirect estimate of tissue oxygenation, we also analyzed HIF-1α activity in nuclear extracts obtained from kidneys of each species and examined its relationship with plasma oxygen content as reflected by the presence of circulating ferrous PolyHbBv (oxy) as a function of time (Fig. 7). There was a clear inverse relationship between the levels of ferrous PolyHbBv (oxy) and HIF activity in both rat (Fig. 7A, r^2 = 098) and guinea pig (Fig. 7B, r^2 = 0.87) in the first 50 hours after ET with PolyHbBv. Notably, maximum suppression of HIF activity was achieved over the first 10 hours when maximum ferrous PolyHbBv (oxy) was observed in the circulation of both species. Interestingly, by 72 hours post ET, when PolyHbBv (oxy) was cleared from the circulation, there was approximately a 2-fold increase in renal HIF activity in the guinea pig compared to the rat. Our data is consistent with a recent report which showed a dramatic effect of increased oxygen affinity delivery by RBCs on angiogenesis and HIF-1α. Allosteric modulation of RBCs treated with ITPP (allosteric modifier of oxygen affinity) which causes a 7mmHg drop in the RBCs P_{50} leading to considerable

suppression in HIF-1α activity (5- fold) and VEGF (1.29-fold) in endothelial cells subjected to hypoxia (Keida et al., 2007).

Heart and Kidney Histopathology:

To investigate whether the interspecies differences in PolyHbBv oxidation/oxygenation translated into differences in organ pathology, we performed H and E staining and histopathological analysis of heart (Fig. 8) and kidneys (Fig. 9) obtained at baseline (24 hours after surgery), 24, and 72 hours post-ET. Tissues from each species (n=3-5 per treatment per time point) were scored by a veterinary pathologist using a semiquantitative grading system such that mean ± SEM severity scores provide a general evaluation of tissue inflammation (I) and necrosis (N). Rat and guinea pig heart (left ventricle) and kidneys exhibited minimal (0) to mild (1) pathologic response to PolyHbBv at 24 hours post ET in rat and guinea pig heart and kidneys with regard to I and N. Figure 8 (B and D) show mild and focal focal myofibers N in the left ventricle and focal inflammation (inset). Myofiber involvement tended to resolve in both species within 72 hours. Figure 9 (B and D) shows glomeruli in kidneys harvested 24 hours after dosing revealing no glomerular injury in either species. This was also observed in the 72 hour group post ET harvested kidney tissue. No abnormal histopathology was noted in any of the heart or kidneys of animals exchange transfused with albumin (data not shown).

Discussion

Infusion of HBOCs can lead to deleterious effects due to the spontaneous and uncontrolled oxidation of its heme iron. This process can be enhanced by endogenous oxidants, such as H_2O_2 and NO and/or its metabolites in circulation. The rapid conversion of the ferrous (oxygen carrying iron) to the ferric (non-oxygen carrying iron) may compromise the effectiveness and safety of HBOC for at least two reasons: (i) ferric Hb does not bind oxygen and its accumulation can reduce the oxygen-carrying capacity of HBOCs; (ii) ferric Hb in the presence of oxidants can promote and sustain a vicious oxidative cycle that ultimately leads to the loss of highly cytotoxic heme. We previously reported that endogenous and/or exogenous reducing agents such as AA (Dunn et al., 2006) or selenium (Baldwin et al., 2004) can control Hb oxidation reactions *in vitro* and *in vivo* and that these reductants can potentially suppress the untoward consequences of these reactions. In the current work, we tested the hypothesis that oxidation of polymerized bovine Hb would be modulated differentially in the circulations of two species with different reductive capabilities, i.e. with and without the ability to synthesize AA as these differences may impact Hb oxygen carrying capabilities.

Plasma antioxidative status was clearly compromised in guinea pigs following ET as evidenced by the 50% reduction in plasma AA. In contrast, rat plasma AA levels remained slightly above baseline levels until PolyHbBv was cleared from the animal's circulation. This likely reflects the ability of rats to generate sufficient AA to compensate for the loss of AA incurred from the ET and from its utilization during the reduction of PolyHbBv. In addition to AA, urate has been shown to play a significant role in

maintaining the ferrous state of Hb in plasma and RBCs (Ames et al., 1981). However, both rat and guinea pig metabolize urate similarly and maintain mean plasma levels of 9.3 μg/mL and 7.0 μg/mL, respectively (Habu et al., 2003; Mudge et al., 1968). Therefore, the influence of urate in these studies is likely not significant. Moreover, we recently estimated that in rabbits which contain approximate plasma concentrations of AA (50 μM) and urate (30 μM), respectively, AA was kinetically more competent in reducing the oxidized forms (ferric/ferryl) of the infused cross-linked Hb than urate (Dunn et al., 2006).

When taking the oxidative status of PolyHbBv heme iron into account, a disconnect in the pharmacokinetics of ferric and ferrous PolyHbBv becomes apparent in the guinea pig. The *in vivo* oxidation of PolyHbBv in the guinea pig resulted in a 5-fold higher overall exposure ($AUC_{0-\infty}$) to ferric PolyHbBv. Additionally, in the guinea pig, approximately 20% and 40% of the circulating PolyHbBv was oxidized to ferric PolyHbBv by 4 and 36 hours post ET, respectively. These values correspond to earlier *in vitro* autoxidation experiments carried out on PolyHbBv in the absence of added antioxidants (Alayash et al., 2001). Conversely, in the rat, ferric PolyHbBv did not increase until plasma concentrations of PolyHbBv were 20 fold less than the $C_{max.}$ Thus increased levels of ferric PolyHbBv at 48 and 72 hours occur at low total PolyHbBv concentrations. Our data is in agreement with several studies using large volume HBOC administration that documented significant ferric Hb formation in sheep (Lee et al., 1995), rabbits (Dunn et al., 2006) and humans (O'Harra et al., 2001). Additionally, administration of various percentages of oxidized PEGylated-Hb to rats as a 30% ET demonstrated that excess of

10% PEGylated-Hb in the oxidized form (ferric PEGylated-Hb) reduced both kidney and liver oxygen tension (Lindberg et al., 1998). These observations suggest a potential for increased toxicity as a result of diminished oxygen delivery and oxidative side reactions caused by excessive ferric HBOC exposure.

Using MALDI-MS, the current study evaluated the *in vivo* oxidative modification as reflected in the structural stability of the tetrameric component of PolyHbBv, which constitutes 37% in the pre-infused final polymer mixture. The mass spectra from rat and guinea pig plasma at 4 and 24 hours post ET demonstrated stability of the PolyHbBv tetramer in plasma sampled from rats at both early and later time points. However, PolyHbBv tetramer instability occurred in guinea pigs at later sampling time points. This observation is based on the detection of PolyHbBv derived α and β globin chain mass ions in plasma collected from guinea pigs. These ions could not be assigned to RBC derived Hb α and β globin chains. This suggests that PolyHbBv globin chains sustained oxidative changes but likely do not dissociate in the guinea pig. This may be a result of oxidative stress imparted on the protein since tetramer destabilization does not occur in PolyHbBv prior to infusion based on previous extensive mass spectrometry analysis (Buehler PW et al., 2005). Conversely, rat Hb (Fig. 4A-a), guinea pig Hb (Fig. 4B-a), human HbA_0 and non cross-linked PEGylated Hb have been shown to readily dissociate *in vitro* (Iafelice and Perrella et al., 2006). The overall impact of Hb monomer formation *in vivo* could result in acute renal failure based on globin chain deposition in the glomeruli of the kidneys (Savitsky JP et al., 1978).

In spite of some of the reported functional limitations of PolyHbBv, such as incomplete saturation of its OEC at high pO_2, (i.e., 100 mmHg) (see Fig. 6), insensitivity to some allosteric modifiers of Hb function and reduced cooperativity (Alayash, 2001), we show in this study that this Hb retained its oxygen carrying capabilities particularly when the oxidation of its iron was controlled such as the case in the rat presumably by endogenous AA. Conversely, uncontrolled oxidation of this Hb in the guinea pig as evidenced by increased levels of its ferric form and left-shifted OECs may have compromised its ability to carry oxygen. Whether the dramatic interspecies differences in the oxidation/oxygenation profiles documented herein translate into different tissue oxygenation is not yet known. However, analysis of HIF-1α activity in kidney tissues obtained from the rats and guinea pigs may offer some clues. HIF-1α, a major molecular transducer of hypoxia is normally degraded in the presence of oxygen, substrate for prolyl hydroxylase that target HIF-1α to ubiquitination and destruction by the proteasome. By contrast, HIF-1α is stabilized during hypoxia, enabling control of the expression of hundreds of genes. We show for the first time a clear correlation between oxygenation state of Hb during the course of transfusion with renal HIF-1α activity in both species. Moreover, the decrease in oxygen-releasing capacity of PolyHbBv in the guinea pig due to its enhanced oxidation likely contributes to the increase in HIF-1α activity observed after 50 hr post-ET. We are currently assessing HIF-1α protein levels and the expression of several HIF-1 target genes such as erythropoietin (EPO), vascular endothelial growth factor (VEGF) and heme oxygenase (HO-1) in kidney, heart and brain of these animals to better understand the interplay between Hb oxygenation, redox reactions and overall oxygen hemostasis.

The MAP response in both rats and guinea pigs was similar in that elevation occurred immediately after the start of ET. However, the two species differed dramatically in the extent of MAP elevation over baseline values. It is tempting to speculate that AA in rats may have also played part in controlling Hb reaction with NO, a critical molecule in blood pressure control. In addition to the well established role of AA in reducing Hb oxidation, AA may also contribute to Hb other important reactions ie., nitrosative reactions. There has been in recent years a growing interest in endogenous NO storage compounds and the role of AA in inducing NO release from these compounds, particularly low molecular weight S-nitrosthiols such as S-nitrosthiol gluthathione (GSNO) (Foster and Stamler, 2004) or S-nitrosated proteins, such albumin (Grandley et al., 2004). Recent mechanistic studies, using N-nitrosated tryptophan derivative showed that the primary oxidized product of AA, DHA efficiently consumes NO and subsequent release of ascorbyl radical (Kytzia, et al., 2006).

Along with oxidative status of the circulating HBOC, arterial blood pressure response can contribute to decreased efficacy and possible toxicity via reduced blood flow to vital tissues, increased work load on the heart and acute renal injury.

Interestingly, neither the enhanced oxidation nor exaggerated blood pressure responses observed in guinea pigs compared to rats translated into increased tissue pathology. Both rats and guinea pigs demonstrated minimal histopathology in heart and kidney at 24 hours post ET and most findings were resolved by 72 hours post ET. In both species,

myocardial toxicity was limited to single myofiber necrosis of the left ventricle at 24 hours. While the absence of histopathological differences between rat and guinea pig was a surprising finding, it is likely that these observations may in fact provide useful information relative to predicting human safety of HBOCs based on animal data. Additionally this work supports the idea of early biomarker identification detectible in the absence of histopathological evaluation. Even though guinea pigs were unable to control the oxidation of PolyHbBv in the circulation they, like humans have increased tissue antioxidant mechanisms (Nandi et al. 1997), which may have prevented tissue injury in these otherwise normal transfused animals. Once protective antioxidant mechanisms in the tissue are overcome by events such as ischemia followed by reperfusion leading to H_2O_2 and neutrophil released hypochlorus acid accumulation the combination of an oxidized HBOC and tissue oxidant accumulation may become overwhelming.

In summary, we show that rats, unlike guinea pigs, controlled oxidation of the infused cell-free Hb after 50% ET and maintained adequate plasma oxygenation with little or no change in the Hb's P_{50}, due in large part to the presence of adequate circulating AA levels during the first 20 hours post-ET. By contrast, in guinea pigs, Hb oxidation preceded in the plasma at much higher rates likely due to the lack of endogenous sources of AA. The decreased ability of this Hb to carry oxygen due to the increased oxidation of its iron was consistent with the increased HIF-1α activity particularly at later times post-ET. This study has therefore the following implications for the use of HBOCs in clinical development: (i) guinea pig may represent an appropriate species for the early evaluation of HBOC susceptibility to oxidation and destabilization in circulation and may be more

relevant to simulate the use of HBOCs in clinical settings associated with antioxidant depletion such as trauma and diabetes. (ii) endogenous antioxidant mechanisms in plasma, RBCs as well as in tissue should be taken into account when designing animal studies aimed at understanding HBOC oxygenation/oxidation reactions. (iii) co-administration of reducing agents such as AA, may offer a simple strategy to control Hb oxidative side reactions.

References

Alayash AI (2004) Oxygen therapeutics: can we tame haemoglobin? *Nat Rev Drug Discov*. **3**:152-159.

Alayash AI, Summers AG, Wood F and Jia Y (2001) Effects of glutaraldehyde polymerization on oxygen transport and redox properties of bovine hemoglobin. *Arch Biochem Biophys.* **391**:225-234.

Ames BN, Cathcart R, Schwiers E, and Hochstein P (1981) Uric acid provides an antioxidant defense in humans against oxidant- and radical-caused aging and cancer: a hypothesis. *Proc Natl Acad Sci* U S A. **78**:6858-6862.

Ancill RJ (1956) The blood volume of the normal guinea-pig. *J. Physiology* **132**, 496-475.

Baldwin AL, Wiley EB and Alayash AI (2004) Differential effects of sodium selenite in reducing tissue damage caused by three hemoglobin-based oxygen carriers. *J Appl Physiol.* **96**:893-903.

Buehler PW, Boykins RA, Norris S, Freedberg DI and Alayash AI (2005) Structural and functional characterization of glutaraldehyde-polymerized bovine hemoglobin and its isolated fractions. *Anal Chem*. **77**:3466-3478.

Carmichael FJ, Ali ACY, Campbell JA; Langlois SF, Biro GP, Willan AR, Pierce CH, Greenburg AG (2000) A phase I study of oxidized raffinose cross-linked human hemoglobin. *Crit Care Med.* **28**:2283-2292.

Chatterjee IB(1973) Evolution and the biosynthesis of ascorbic acid. *Science* **182**:1271-1272.

Dunne J, Caron A, Menu P, Alayash AI, Buehler PW, Wilson MT, Silaghi-Dumitrescu R, Faivre B and Cooper CE (2006) Ascorbate removes key precursors to oxidative damage by cell-free haemoglobin in vitro and in vivo. *Biochem J*. **399**:513-524.

Foster MW and Stamler JS (2004) New insights into protein S-nitrosylation. Mitochondria as a model system. *J Biol Chem.* **279**:25891-25897.

Garrick LM, Sharma VS, McDonald MJ, Ranney HM (1975) Rat haemoglobin heterogeneity. Two structurally distinct alpha chains and functional behaviour of selected components. Biochem J. **149**:245-258.

Grandley, R.E., Tyurin, V.A., Huang, W, Huang, Arroyo A, Daftary A, Harger, G, Jiang J, Pitt B, Taylor RN, Hubel CA, Kagan VE (2005) S-Nitrosoalbumin-mediated relaxation is enhanced by ascorbate and copper: Effects in pregnancy and preeclampsia plasma. *Hypertension* **45**:21-27

Hayashi A, Suzuki T and Shin M (1973) An enzymic reduction system for metmyoglobin and methemoglobin, and its application to functional studies of oxygen carriers. *Biochim Biophys Acta*. **310**:309-316.

Habu Y, Yano I, Takeuchi A, Saito H, Okuda M, Fukatsu A and Inui KI (2003) Decreased activity of basolateral organic ion transports in hyperuricemic rat kidney: roles of organic ion transporters, rOAT1, rOAT3 and rOCT2. *Biochem Pharmacol*. **66**:1107-1114.

Iafelice R, Cristoni S, Caccia D, Russo R, Rossi-Bernardi L, Lowe KC and Perrella M (2006) Identification of the sites of deoxy haemaglobin pegylation. Biochem J. **403**:189-196.

Kieda C, Greferath R, Crola Da Silva C, Fylaktakidou KC, Lehn JM, and Nicolau C (2006) Suppression of hypoxia-induced HIF-1alpha and of angiogenesis in endothelial cells by myo-inositol trispyrophosphate-treated erythrocytes. *Proc Natl Acad Sci* U S A. **103**:15576-15581.

Kim HW and Greenburg AG (2004) Artificial oxygen carriers as red blood cell substitutes: a selected review and current status. *Artif Organs*. **28**:813-828.

Kytzia, A., Korth, H-G., Sustmann, R., De Groot, H., and Kirsch, M. (2006) On the mechanism of the ascorbic acid-induced release of nitric oxide from N-nitrosated

tryptophan derivatives: scavenging of NO by ascorbyl radicals. Chemistry. **12**:8786-8797.

Lee HB and Blaufox MD (1985) Blood volume in the rat. *J of Nuclear Medicine* **26**: 72-76.

Lee R, Neya K, Svizzero TA and Vlahakes GJ (1995) Limitations of the efficacy of hemoglobin-based oxygen-carrying solutions. *J Appl Physiol.* **79**:236-242.

Linberg R, Conover CD, Shum KL and Shorr RGL (1998) Hemoglobin based oxygen carriers: how much methemoglobin is too much? Artif Cells Blood Substit Immobil Biotechnol. **26**:133-148.

May JM, Qu ZC, and Cobb CE (2004) Human erythrocyte recycling of ascorbic acid: relative contributions from the ascorbate free radical and dehydroascorbic acid *J Biol Chem* **279**: 14975-14982.

Mudge GH, Cucchi J, Platts M, O'Connell JM and Berndt WO (1968) Renal excretion of uric acid in the dog. *Am J Physiol.* **215**:404-410.

Nagababu E, Ramasamy S, Rifkind JM, Jia Y, and Alayash AI (2002) Site-specific cross-linking of human and bovine hemoglobins differentially alters oxygen binding and redox

side reactions producing rhombic heme and heme degradation. *Biochemistry* **41**:7407-7415.

Nandi A, Mukhopadhyay CK, Ghosh MK, Chattopadhyay DJ and Chatterjee IB (1997) Evolutionary significance of vitamin C biosynthesis in terrestrial vertebrates. *Free Radic Biol Med.* **22**:1047-1054.

O'Harra JF, Colburn WA, Tetzlaff JE, Novick AC, Angermeier KW and Schubert A (2001) Hemoglobin and methemoglobin concentrations after large-dose infusions of diaspirin cross-linked hemoglobin. *Anesth Analg* **92**: 44-48.

Przybelski RJ, Daily EK, Kisicki JC, Mattia-Goldberg C, Bounds M, ColburnWA (1996) Phase I study of the safety and pharmacologic effects of diaspirin cross-linked hemoglobin solution. *Crit Care Med.* **24**:1993-2000.

Riess JG (2001) Oxygen carriers ("blood substitutes")--raison d'etre, chemistry, and some physiology. *Chem Rev.* **101**:2797-2920.

Savitsky JP, Doczi J, Black J and Arnold JD (1978) A clinical safety trial of stroma free hemoglobin. *Clinical Pharmacology and Therapeutics* **23**:73-80.

Sloan EP, Koenigsberg M, Gens D, Cipolle M, Runge J, Mallory MN, Rodman G. Jr (1999) Diaspirin cross-linked hemoglobin (DCLHb) in the treatment of severe traumatic hemorrhagic shock: a randomized controlled efficacy trial. *JAMA*. **282**:1857-1864.

Su D, May JM, Koury MJ, and Asard H (2006) Human erythrocyte membranes contain a cytochrome b561 that may be involved in extracellular ascorbate recycling. *J Biol Chem.* **281**:39852-39859.

Winterbourn CC (1985) In CRC Handbook of Methods of Oxygen Radical Research; Greenwald, RA Ed.; CRC Press: Boca Raton FL; pp 137-141.

Footnotes:

The findings and conclusions in this article have not been formally disseminated by the Food and Drug Administration and should not be construed to represent any Agency determination or policy. We thank Dr. Paul Yeh for performing DNA transbinding assessment of HIF-1α and Ms. Francine Wood for performing oxygen equilibrium measurements. This work was funded by a FDA/CBER Unmet Needs Award.

JPET Fast Forward. Published on July 10, 2007 as DOI: 10.1124/jpet.107.126409
This article has not been copyedited and formatted. The final version may differ from this version.

Legends for figures

Fig. 1 – Plasma ascorbic acid and hematocrit in rat and guinea pig following PolyHbBv exchange transfusion

(A) Pre and post-exchange transfusion plasma ascorbic acid concentrations in the rat (-○-) and guinea pig (-●-). (B) Pre and post-exchange transfusion hematocrit in the rat (filled bars) and the guinea pig (open bars). Values are reported as μM ± SEM. Significant differences ($P<0.05$) between rat and guinea pig are denoted by ‡, while significant differences from baseline values are denoted by *. (n = 5-6 animals per species per time point)

Fig. 2 – Log-linear plasma concentration versus time profiles of PolyHbBv in rats and guinea pigs

Plasma concentrations of total PolyHbBv (-■-), ferrous PolyHbBv (-●-), and % plasma ferric PolyHbBv (-○-) at time points from the end of exchange transfusion until 72 hours in the rat (A) and guinea pig (B). Convergence of dotted and dashed lines indicates the period of greatest ferric PolyHbBv exposure. The pharmacokinetic estimates derived from this data are shown in Table 1.

Fig. 3 –Size exclusion chromatography patterns of plasma PolyHbBv over time in the rat and guinea pig.

(A) Shows a representative (single animal) pattern of tetrameric and multi-tetrameric fractions in PolyHbBv as they exist in the plasma of the rat over time. (B) Shows a

representative (single animal) pattern of tetrameric and multi-tetrameric fractions in PolyHbBv as they exist in the plasma of the guinea pig over time. In each case plasma samples (50 uL) were run on BioSep-SEC-S3000 (600 mm x 7.5 mm) SEC column. The running buffer consisted of 0.1 M NaH_2PO_4, pH 6.5, pumped at rate of 0.5 mL/min and the absorbance was monitored at 405 nm.

Fig. 4 A and B – MALDI-MS evaluation of HbG globin chain destabilization in plasma sampled from rat and guinea pig.

(4A-a) Shows the MALDI-MS spectra of rat red blood cell hemoglobin obtained from rats whole blood sampled at baseline. The $[M+H]^{1+}$ ion at *m/z* = 15201.6 and *m/z* = 15851.51 represent the primary α and β globin chain ions in rat red cells and serves as a control for the presence of red cell hemoglobin which could be present in plasma samples (a and b). (4A-b) Shows the MALDI-MS spectra of rat plasma sampled at 4 hours post exchange transfusion. The $[M+H]^{1+}$ ions denoted α* at *m/z* = 15328.46, β* *m/z* = 16110.63 and α*- α* m/z = 30940.17, represent the tetrameric fraction of PolyHbBv's α, β and α - α cross-linked species. (4A-c) Shows the MALDI-MS spectra of rat plasma sampled at 24 hours post exchange transfusion. The $[M+H]^{1+}$ ions denoted α* at *m/z* = 15285.00, β* *m/z* = 16108.70 and α*- α* m/z = 30932.26, represent the tetrameric fraction of PolyHbBv's α, β and α - α cross-linked species. The arrow indicates the $[M+H]^{1+}$ ion for albumin, this ion becomes more abundant (less suppressed) as PolyHbBv is cleared from the plasma.

(4B-a) Shows the MALDI-MS spectra of guinea pig red blood cell hemoglobin obtained from guinea pig whole blood sampled at baseline. The $[M+H]^{1+}$ ion at *m/z* = 15228..59 and *m/z* = 15921.00 represent the primary α and β globin chain ions in guinea pig red cell hemoglobin and serves as a control for the presence red cell hemoglobin which could be present in plasma samples (a and b). (4B-b) Shows the MALDI-MS spectra of guinea pig plasma sampled at 4 hours post exchange transfusion. The $[M+H]^{1+}$ ions denoted α* at *m/z* = 15160.21, β* *m/z* = 16093.84 and α*- α* m/z = 31025.1, represent the tetrameric fraction of PolyHbBv α, β (shown in blue in the full spectra and inset) and α - α cross-linked species. (4B-c) Shows the MALDI-MS spectra of guinea pig plasma sampled at 24 hours post exchange transfusion. The $[M+H]^{1+}$ ions denoted α* at *m/z* = 15250.81, β* *m/z* = 16125.87 and α*- α* m/z = 31009.68, represent the tetrameric fraction of PolyHbBv's α, β (shown in red in the full spectra and inset) and α - α cross-linked species. The increase in intensity of the α* ion could not be assigned to the guinea pigs own red cell Hb (m/z = 15228.59), thus the intensity increase is consistent with α - α cross-link destabilization. The arrow indicates the $[M+H]^{1+}$ ion for albumin, this ion becomes more abundant (less suppressed) as PolyHbBv is cleared from the plasma.

Fig. 5 – Cardiovascular effects of PolyHbBv in the rat and guinea pig. (A) Percent change from baseline in mean arterial pressure (MAP) in the guinea pig (-■-) and rat (-●-). MAP increase compared to baseline was 20% in rats compared to 50% in guinea pigs Values represent mean ± SEM. (B) Percent change from baseline in heart rate response in rat (-■-) and guinea pig (-●-). Measurements were recorded continuously and plotted at two minute intervals. Significant differences ($P < 0.05$) were observed in both the rat and

guinea pig over the entire two hour period post transfusion compared to baseline. (n = 5 for each species)

Fig. 6: **Oxygen equilibrium curves (OECs) for Figure 6**: **Oxygen equilibrium curves (OECs) for PolyHbBv in rat and guinea pig plasma**: Oxygen equilibrium curves for samples obtained post transfusion from plasma of rats (A) and guinea pigs (B) at specific time intervals are shown. OECs were determined by automated Hemox analyzer at 37C. All samples contained approximatly 60 μM heme in a 0.01 M phosphate buffer containing 0.1 M NaCl) (pH 7.4). Antifoaming agent and Hayashi reduction reagents (see materials and methods) were added to the buffer. Results are expressed as percentages of oxygen saturation vs. partial pressure of oxygen. P_{50} values were obtained from these curves after correction for the incomplete saturation OECs at 100 mmHg (see material and methods).

Fig. 7 – Correlation between the levels of PolyHbBv (oxy) and HIF-1αα DNA binding activity in kidneys from rats and guinea pigs. Ferrous form of PolyHbBv (-■-) measured in plasma samples taken from rats (A) and guinea pigs (B) plotted a function of HIF-1α activity as measured by ELISA-based method (see materials and methods) and time (hours) post transfusion with PolyHbBv.

Fig. 8 – Heart histopathological evaluation of rat and guinea pig tissue after PolyHbBv exchange transfusion.

Hematoxylin-eosin stained heart harvested at baseline (24 hours after surgery) and 24 hours post exchange with PolyHbBv in rat (A and B, respectively) and guinea pig (C and D, respectively). The black arrows indicate areas of pathology. In the rat heart (B) single necrotic myofibers are observed in the left ventricle, (B-inset) shows a small inflammatory lesion in the wall of the left ventricle. In the guinea pig heart (D) areas of necrotic myofibers are seen in the apical region of the left ventricle. These findings were mild and in some cases not observed in animals. Resolution was generally achieved by 72 hours post exchange.

Fig. 9 – Kidney histopathological evaluation of rat and guinea pig tissue after PolyHbBv exchange transfusion.

Hematoxylin-eosin stained kidney harvested at baseline (24 hours after surgery) and 24 hours post exchange with PolyHbBv in rat (A and B, respectively) and guinea pig (C and D, respectively) demonstrate no glomerular damage in either the rat or the guinea pig.

JPET Fast Forward. Published on July 10, 2007 as DOI: 10.1124/jpet.107.126409
This article has not been copyedited and formatted. The final version may differ from this version.

Table 1. Pharmacokinetic parameter estimates following PolyHbBv transfusion

Estimates (Rat)	**Total PolyHbBv**	**ferrous PolyHbBv**	**ferric PolyHbBv**
Dose (mg)	1197 ± 104	1112 ± 97.9	84.58 ± 6.03
	(3122 ± 55.0 mg/kg)	(2900 ± 55.0 mg/kg)	(222 ± 0.00 mg/kg)
C_{max} (mg • mL^{-1})	42.4 ± 1.65	41.5 ± 1.55	0.94 ± 0.4
T_{max} (hr)	(0.20 ± 0.0 14)	(0.20 ± 0.014)	(0.20 ± 0.014)
$AUC_{0-\infty}$ (mg hr mL^{-1})	824.3 ± 32.6	774.2 ± 42.7	54.01 ± 10.8
Cl (mL • hr^{-1})	1.45 ± 0.0994	1.55 ± 0.115	
Vss (mL)	31.7 ± 7.97	37.9 ± 16.0	
t½ (hr)	15.6 ± 1.92	13.4 ± 2.14	
$MRT_{i.v.}$ (hr)	21.1 ± 4.29	18.9 ± 4.69	
Estimates (Guinea pig)	**Total PolyHbBv**	**ferrous PolyHbBv**	**ferric PolyHbBv**
Dose (mg)	1186 ± 49.5	1117 ± 38.2	63.32 ± 5.19
	(3272 ± 106 mg/kg)	(3143 ± 70.1 mg/kg)	(188.8 ± 15.6 mg/kg)
C_{max} (mg • mL^{-1})	40.0 ± 2.22	39.4 ± 2.22	4.10 ± 1.0
T_{max} (hr)	(0.19 ± 0.01)	(0.19 ± 0.01)	12
$AUC_{0-\infty}$ (mg • hr • mL^{-1})	788.1 ± 90.6	512.8 ± 67.5	272.0 ± 53.0
Cl (mL • hr^{-1})	1.86 ± 0.31	2.43 ± 0.31	
Vss (mL)	45.3 ± 6.1	49.8 ± 6.1	
t½ (hr)	15.7 ± 0.64	12.9 ± 0.65	
$MRT_{i.v.}$ (hr)	25.1 ± 1.87	20.7 ± 1.49	

Figure 1

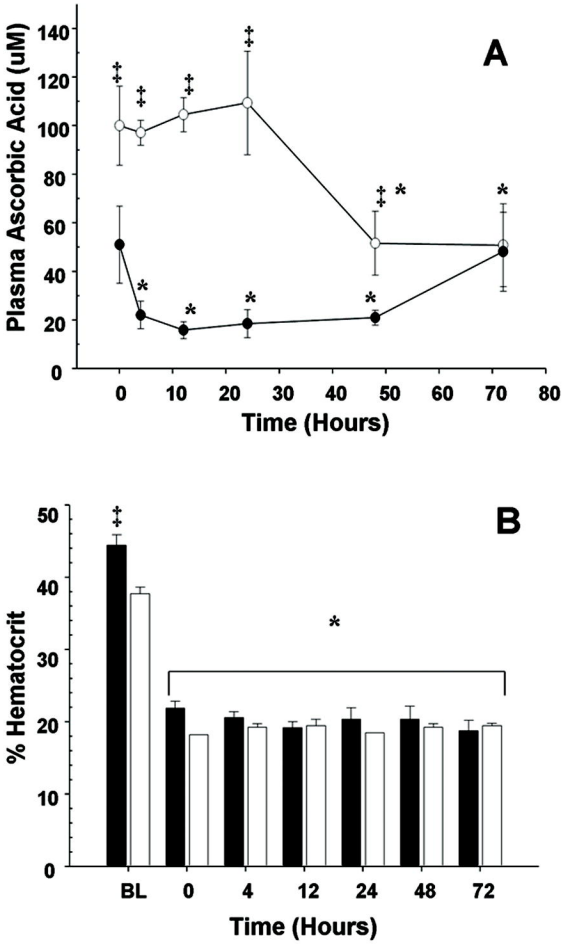
A
Plasma Ascorbic Acid (uM)
140
120
100
80
60
40
20
0
0
10
20
30
40
50
60
70
80
Time (Hours)
B
% Hematocrit
50
40
30
20
10
0
BL
0
4
12
24
48
72
Time (Hours)

Figure 2

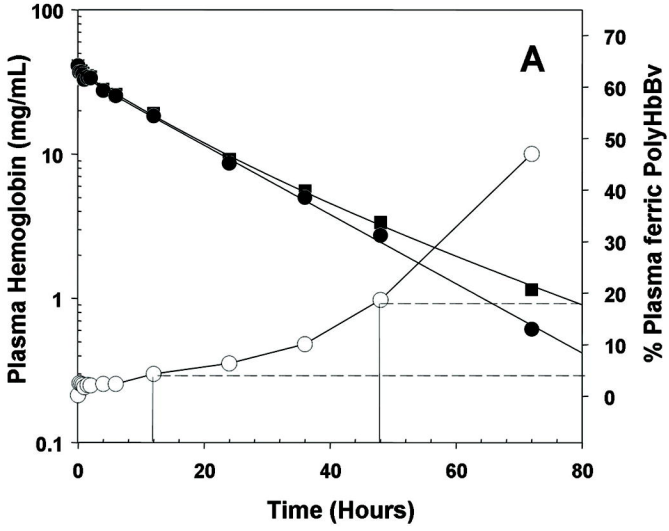
A
Plasma Hemoglobin (mg/mL)
% Plasma ferric PolyHbBv
Time (Hours)
100
10
1
0.1
70
60
50
40
30
20
10
0
0
20
40
60
80

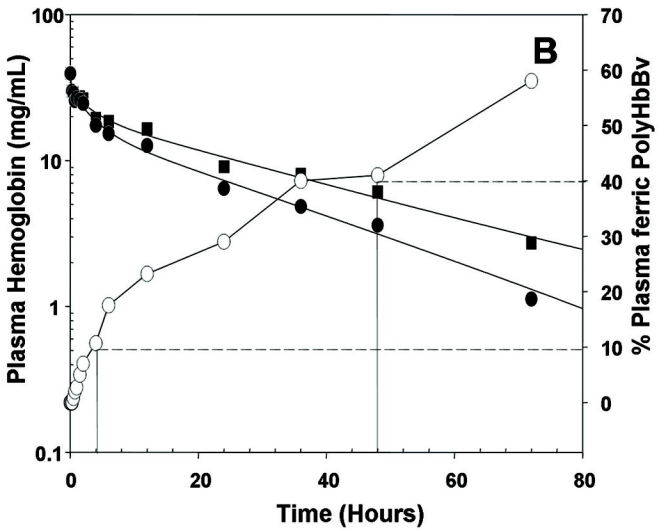
B
Plasma Hemoglobin (mg/mL)
% Plasma ferric PolyHbBv
Time (Hours)
100
10
1
0.1
70
60
50
40
30
20
10
0
0
20
40
60
80

Figure 3

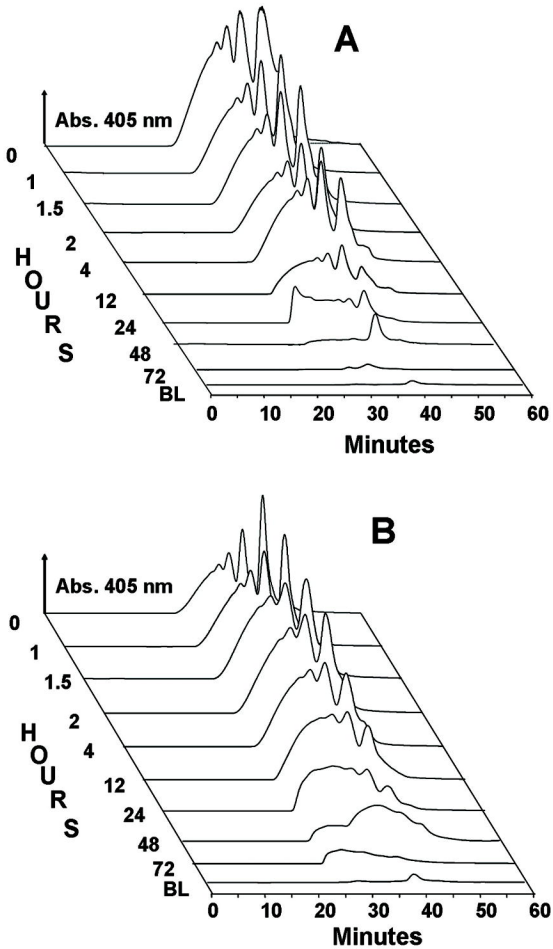
A
Abs. 405 nm
0
1
1.5
2
4
12
24
48
72
BL
HOURS
0
10
20
30
40
50
60
Minutes
B
Abs. 405 nm
0
1
1.5
2
4
12
24
48
72
BL
HOURS
0
10
20
30
40
50
60
Minutes

Figure 4A

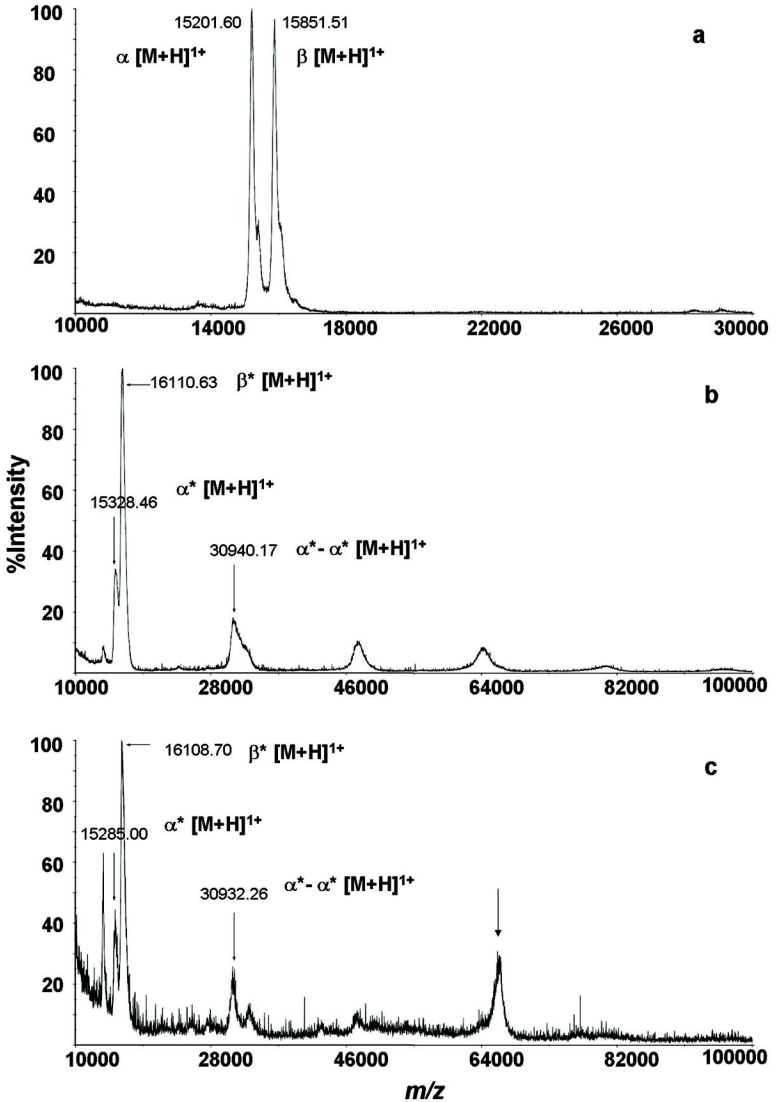
a
15201.60
15851.51
α [M+H]1+
β [M+H]1+
b
16110.63 β* [M+H]1+
α* [M+H]1+
15328.46
30940.17 α*- α* [M+H]1+
%Intensity
c
16108.70 β* [M+H]1+
α* [M+H]1+
15285.00
30932.26 α*- α* [M+H]1+
m/z

Figure 4B

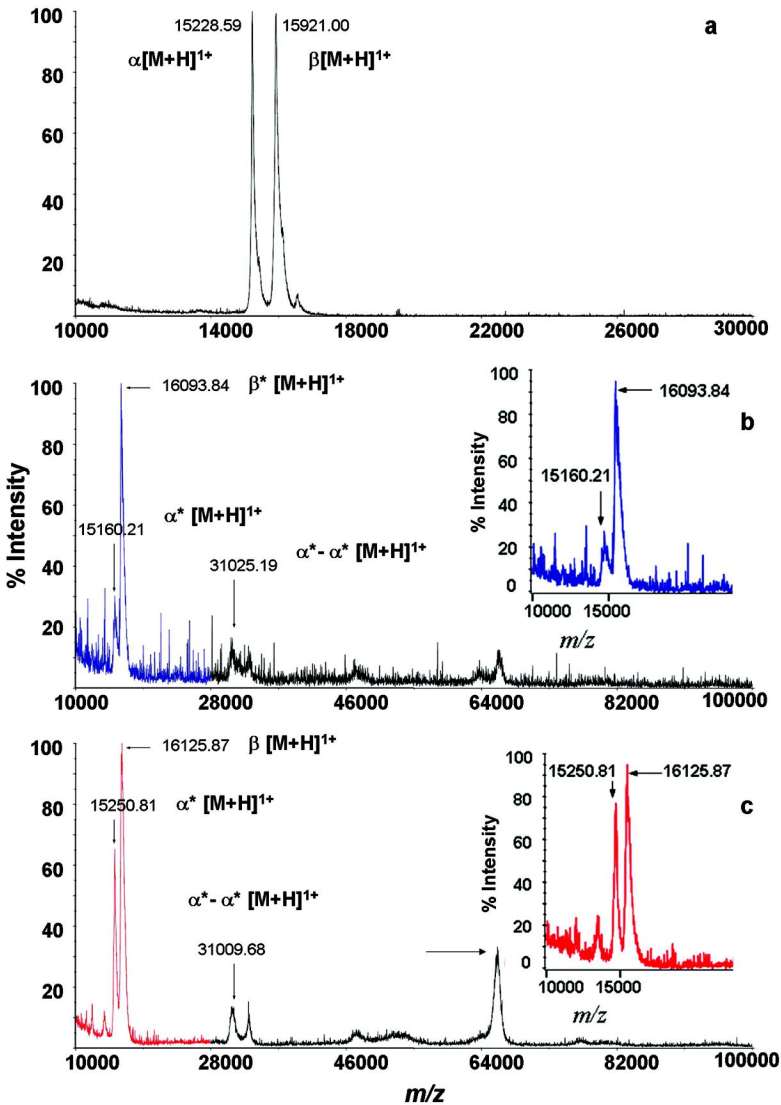
a
15228.59
15921.00
α[M+H]1+
β[M+H]1+
100
80
60
40
20
10000
14000
18000
22000
26000
30000
b
16093.84
β* [M+H]1+
15160.21
α* [M+H]1+
α*- α* [M+H]1+
31025.19
% Intensity
10000
28000
46000
64000
82000
100000
m/z
c
16125.87
β [M+H]1+
15250.81
α* [M+H]1+
α*- α* [M+H]1+
31009.68
% Intensity
m/z

Figure 5

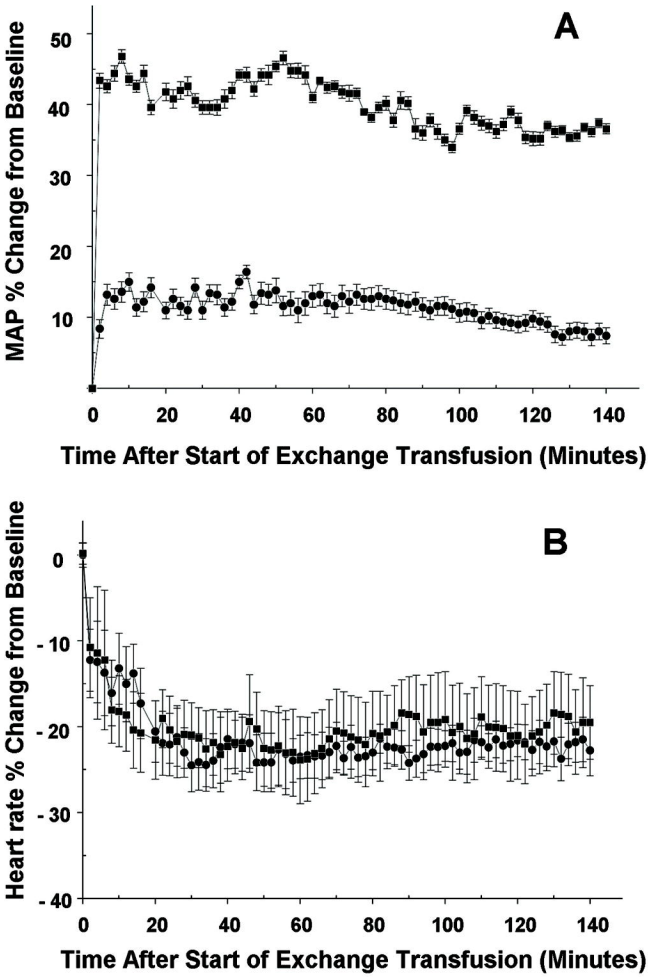
A
MAP % Change from Baseline
50
40
30
20
10
0
20
40
60
80
100
120
140
Time After Start of Exchange Transfusion (Minutes)
B
Heart rate % Change from Baseline
0
- 10
- 20
- 30
- 40
0
20
40
60
80
100
120
140
Time After Start of Exchange Transfusion (Minutes)

Figure 6

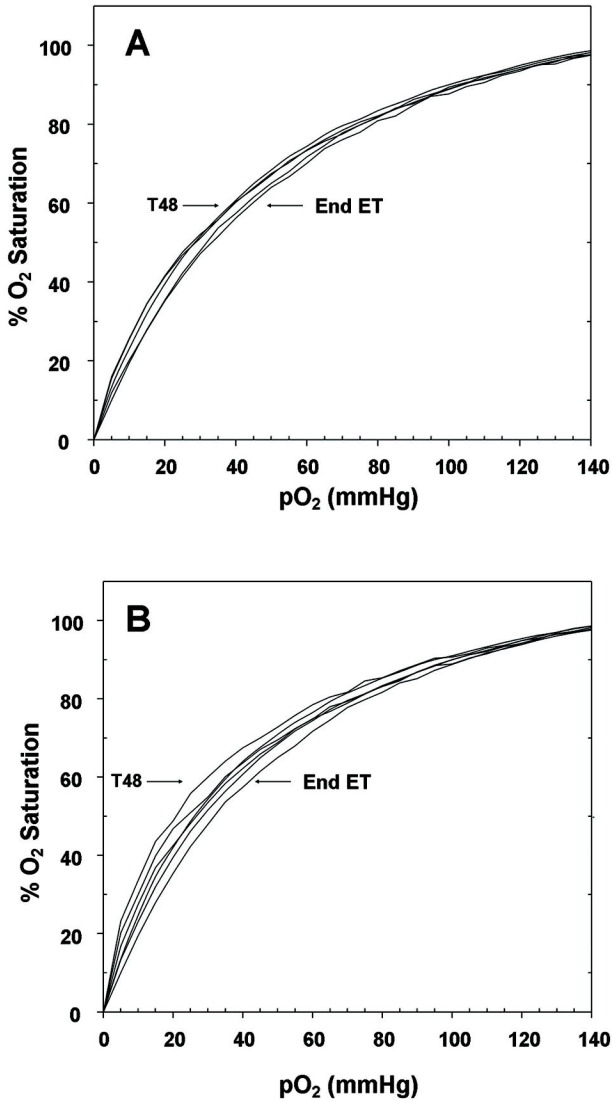
A
100
80
60
40
20
0
% O_2 Saturation
T48
End ET
0
20
40
60
80
100
120
140
pO_2 (mmHg)
B
100
80
60
40
20
0
% O_2 Saturation
T48
End ET
0
20
40
60
80
100
120
140
pO_2 (mmHg)

Figure 7

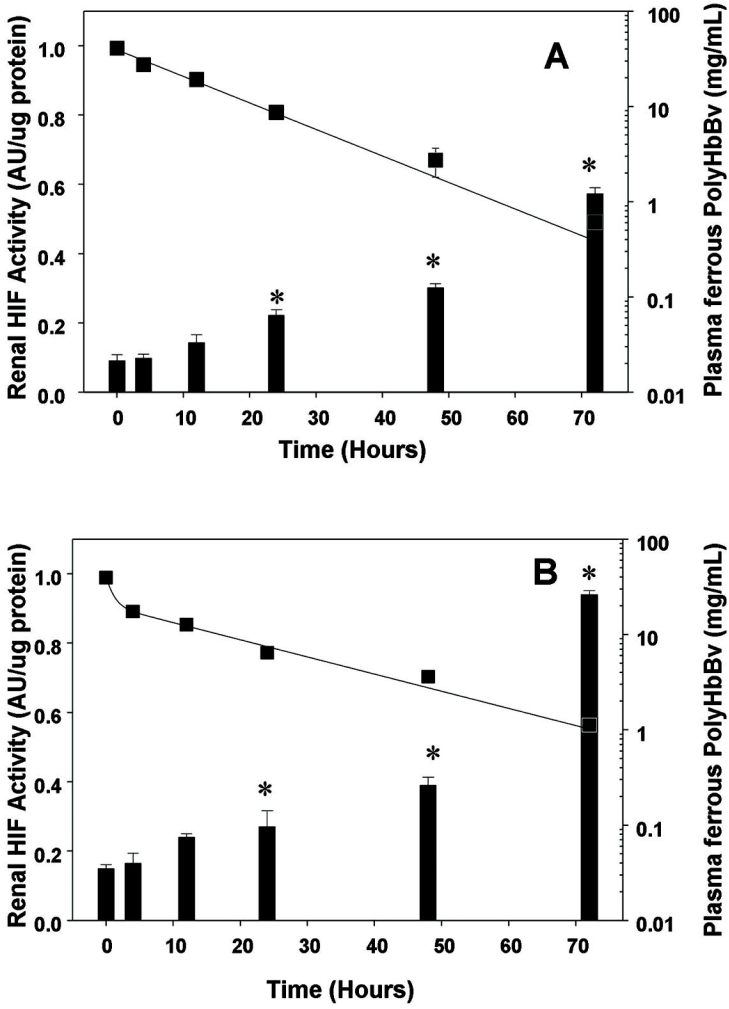
A
B
Renal HIF Activity (AU/ug protein)
Plasma ferrous PolyHbBv (mg/mL)
Time (Hours)
0.0
0.2
0.4
0.6
0.8
1.0
0.01
0.1
1
10
100
0
10
20
30
40
50
60
70
*

Figure 8

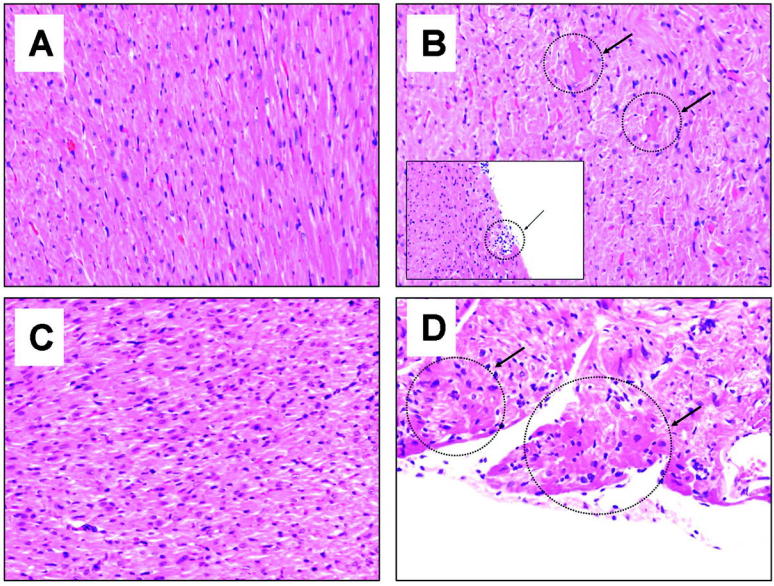

Figure 9